

NEUTRINOS FROM GAMMA-RAY BURSTS: PROPAGATION OF COSMIC RAYS IN THEIR HOST GALAXIES

ZI-YI WANG^{1,2}, XIANG-YU WANG^{1,2}, JUN-FENG WANG³

¹ School of Astronomy and Space Science, Nanjing University, Nanjing, 210093, China; xywang@nju.edu.cn

² Key laboratory of Modern Astronomy and Astrophysics (Nanjing University), Ministry of Education, Nanjing 210093, China

³ Department of Astronomy and Institute of Theoretical Physics and Astrophysics, Xiamen University, Xiamen, Fujian 361005, China

Draft version June 28, 2021

ABSTRACT

Gamma-ray bursts (GRBs) are proposed as candidate sources of ultra-high energy cosmic rays (UHECRs). We study the possibility that the PeV neutrinos recently observed by IceCube are produced by GRB cosmic rays interacting with the interstellar gas in the host galaxies. By studying the relation between the X-ray absorption column density N_H and the surface star-formation rate of GRB host galaxies, we find that N_H is a good indicator of the surface gas density of the host galaxies. Then we are able to calculate the neutrino production efficiency of CRs for GRBs with known N_H . We collect a sample of GRBs that have both measurements of N_H and accurate gamma-ray fluence, and attempt to calculate the accumulated neutrino flux based on the current knowledge about GRBs and their host galaxies. When the CR intensity produced by GRBs is normalized with the observed UHECR flux above $\sim 10^{19}$ eV, the accumulated neutrino flux at PeV energies is estimated to be about $(0.3 \pm 0.2) \times 10^{-8} \text{ GeV cm}^{-2} \text{ s}^{-1} \text{ sr}^{-1}$ (per flavor) under the assumption that GRB energy production rate follows the cosmic star-formation rate and the favorable assumption about the CR diffusion coefficient. This flux is insufficient to account for the IceCube observations, but the estimate suffers from some assumptions in the calculation and thus we can not rule out this scenario at present.

Subject headings: neutrinos – gamma-ray: bursts

1. INTRODUCTION

Gamma-ray bursts (GRBs) have been proposed as a potential origin of ultra-high-energy cosmic rays (UHECRs) (e.g., Waxman 1995; Vietri 1995; Milgrom and Usov 1995). High-energy neutrinos are thought to be a useful messenger to probe CR acceleration in GRBs, as they are predicted to be produced in the dissipative fireballs, where cosmic-ray protons interact with fireball gamma-ray photons through photopion process (e.g., Waxman & Bahcall 1997; Guetta et al. 2004; Dermer & Atoyan 2006; Murase et al. 2006; Wang & Dai 2009). However, search for high-energy neutrinos in coincident with GRBs using IceCube has failed to find any associated neutrinos so far (Abbasi et al. 2012; Aartsen et al. 2015). The non-detection has put stringent constraints on the neutrino production efficiency and fireball properties of GRBs (He et al. 2012; Zhang & Kumar 2013; Gao et al. 2013; Yacobi et al. 2014). Because the low neutrino flux could be simply due to a low efficiency in converting CRs to neutrinos, as expected in some GRB models with large dissipation radius, one can not rule out CR acceleration in GRBs with the non-detection of neutrinos.

CRs accelerated by GRBs will finally escape from the source and enter the interstellar space of the host galaxy. The proton-proton collisions between CRs and nuclei in the interstellar medium will also produce high-energy neutrinos. Recently, IceCube Collaboration reported the detection of extraterrestrial TeV-PeV neutrinos with a best-fit flux of $E_\nu^2 \Phi_\nu = (0.95 \pm 0.3) \times 10^{-8} \text{ GeV cm}^{-2} \text{ s}^{-1} \text{ sr}^{-1}$ per flavor (Aartsen et al. 2014). Noting the coincidence between the IceCube neutrino flux and the Waxman-Bahcall bound ($\sim 10^{-8} \text{ GeV cm}^{-2} \text{ s}^{-1} \text{ sr}^{-1}$) derived from the flux of UHECRs above 10^{19} eV, some authors suggest that IceCube neutrinos may be produced by the same source responsible these UHECRs (Waxman 2013; Katz et al. 2013). As GRBs are one candidate source of UHECRs, one may wonder whether neutrinos resulted from the CR collisions with the ISM in the host

galaxy can explain the IceCube observations (Waxman 2013, Wang et al. 2014). In this paper, we study this interesting possibility by perform a calculation of the expected neutrino flux with the knowledge about the properties of GRBs and their host galaxies.

One key unknown factor that decides the neutrino flux from GRB host galaxies is the pion production efficiency, i.e. the energy loss of CR protons into pions due to collisions with the ISM of the host galaxy. CRs interact with the ISM along their path before escape, so this efficiency relates with the gas column density that CRs traversed. As CRs are transported outward by galactic winds, the gas surface density Σ_g represents an averaged column density of matter that CRs traversed. However, for most GRBs, we do not have measurements of Σ_g at the GRB explosion site as GRB hosts are hardly spatially resolved. We note that the X-ray absorption column density N_H , inferred from the X-ray observations of the prompt and afterglow emission, has a similar role, but N_H reflects the column density along the direction of the line of sight (rather than the averaged gas column density). Moreover, the value of N_H is derived assuming solar metallicity for the absorbing gas, while GRBs seem to occur preferentially in low metallicity galaxies (Stanek et al. 2006; Prieto et al. 2008). The X-ray absorption, as measured with Swift/XRT observations, mainly takes place through inner shell electrons of metals, thus it is linked to the metallicity of the ISM in the host galaxies. If GRB host galaxies have lower metallicity, the true absorbing gas column density should be higher than the quoted values obtained from fitting X-ray afterglows, considering this metallicity difference. We thus first study how well N_H can trace the gas surface density Σ_g in §2. We find that N_H is well correlated with the surface star-formation rate (Σ_{SFR}) of the host galaxies. Then taking into account the Kennicutt - Schmidt law that relates the surface gas density and the surface star-formation rate (Kennicutt 1998), we obtain a relation between N_H and Σ_g . Once Σ_g is known for each GRB, we can

calculate the neutrino production efficiency and further calculate the accumulated neutrino flux from all GRB host galaxies (§3).

2. THE RELATIONS BETWEEN N_H AND Σ_G

Because we have very few measurements of Σ_{SFR} , but have measurement of N_H for many GRBs, we study whether N_H are correlated with Σ_{SFR} and act as an indicator of the gas surface density. We collect the GRB hosts that have spatially resolved observations from literatures (Svensson et al. 2010; Fruchter et al. 2006; Savaglio et al. 2009), which are given in Table 1. The total SFR and 80% light radius of these hosts R_{80} are obtained in these observations. By comparing the 80% light radius and half light radius of some GRB hosts that are spatially resolved (Fruchter et al. 2006; Kelly et al. 2014), we find that $R_{80} \simeq 2R_{50}$. Converting 80% light radius to the half-light radius R_{50} with $R_{80} = 2R_{50}$, we calculate the surface star-formation rates Σ_{SFR} . With a sample of 18 GRBs that have both measurements of N_H from the XRT data of Swift observations and Σ_{SFR} of their host galaxies, we then study the relation between N_H and Σ_{SFR} . Through the ordinary least-squares (OLS) bisector fitting¹ (Isobe et al. 1990), we find that

$$\Sigma_{\text{SFR}} = 10^{-1.89 \pm 0.27} \left(\frac{N_H}{10^{21} \text{cm}^{-2}} \right)^{1.42 \pm 0.25} M_{\odot} \text{yr}^{-1} \text{kpc}^{-2} \quad (1)$$

with a correlation coefficient of $r = 0.756$ and a null hypothesis probability of $p = 7.09 \times 10^{-4}$, indicating a good correlation. The result of the fit is shown in the left panel of Fig.1. Considering the Kennicutt-Schmidt law between the surface SFR and the surface density of molecular plus atomic gas (Kennicutt 1998), i.e.,

$$\Sigma_{\text{SFR}} = (2.5 \pm 0.7) \times 10^{-4} \left(\frac{\Sigma_g}{1 M_{\odot} \text{pc}^{-2}} \right)^{1.4 \pm 0.15} M_{\odot} \text{yr}^{-1} \text{kpc}^{-2}, \quad (2)$$

we get

$$\Sigma_g = (2.1 \pm 1.0) \times 10^{21} \left(\frac{N_H}{10^{21} \text{cm}^{-2}} \right)^{1.01 \pm 0.21} m_H \text{cm}^{-2}, \quad (3)$$

where m_H is the mass of the hydrogen atom. The roughly linear relation between Σ_g and N_H suggests that N_H is a good indicator of the gas surface density Σ_g . Note that N_H is derived assuming solar metallicity for the absorbing gas. Since GRB host galaxies usually have lower metallicity, the true absorbing gas column density should be corrected by the metallicity effect. The coefficient 2.1 ± 1.0 may reflect such a correction.

We also study whether N_H are correlated with the total SFRs of the host galaxies. We collect 35 GRBs in total that have measurements of N_H and total SFRs, which are also listed in Table 1. Through the OLS bisector fitting of the data of N_H and SFR, we find that

$$\text{SFR} = 10^{-0.63 \pm 0.23} \left(\frac{N_H}{10^{21} \text{cm}^{-2}} \right)^{1.55 \pm 0.26} M_{\odot} \text{yr}^{-1}, \quad (4)$$

with a correlation coefficient of $r = 0.5576$ and a null hypothesis probability $p = 0.0014$, which indicates a tight positive correlation. The result of the fitting is shown in the right panel of Fig.1. With this relation, we can infer the SFR of GRB hosts with N_H for each GRB in our sample, which will be used to compute the galactic wind velocity in §3.1.

¹ Since our goal is to estimate the functional relation between N_H and Σ_{SFR} , and it is not clear which variable is causative. Therefore, the OLS bisector fitting which treat the variables symmetrically should be used, according to Isobe et al. (1990).

3. NEUTRINO FLUX FROM GRB HOST GALAXIES

3.1. The pion production efficiency

The GRB accelerated CR protons travel through the host galaxy and produce high-energy neutrinos via proton-proton(pp)-collisions with its interstellar medium (ISM). The collisions produce charged pions, which decay to neutrinos ($\pi^+ \rightarrow \nu_{\mu} \bar{\nu}_{\mu} \nu_e e^+$, $\pi^- \rightarrow \bar{\nu}_{\mu} \nu_{\mu} \bar{\nu}_e e^-$). Meanwhile, CRs can escape out of the galaxy through diffusion or galactic wind advection. These two competing processes (i.e. collision and escape) regulate the efficiency of the pion-production of CRs, which can be described by $f_{\pi} = 1 - \exp(-t_{\text{esc}}/t_{\text{loss}})$, where t_{loss} is the energy-loss time of CRs via (pp) collisions and t_{esc} is the escape time of CRs. The pp -collision energy loss time is $t_{\text{loss}} = (\kappa n \sigma_{pp} c)^{-1} = (\kappa \Sigma_g \sigma_{pp} c/l)^{-1}$, where $\kappa \simeq 0.5$ is the inelasticity, n is the gas number density, l is the scale height of the gaseous disc of the galaxy. σ_{pp} is the pp -collision inelastic cross-section, which slightly increases with the proton energy, given by $\sigma_{pp} = (34.3 + 1.88L + 0.25L^2) \times$

$\left[1 - \left(\frac{1.22 \times 10^{-6}}{E_p/1 \text{GeV}} \right)^4 \right]^2$ mb where $L = \log \left(\frac{E_p}{1 \text{TeV}} \right)$ (Kelner et al. 2006). Thus, the collision energy loss time is $t_{\text{loss}} = 5.4 \times 10^6 \text{yr} \frac{l}{500 \text{pc}} \left(\frac{\Sigma_g}{0.01 \text{gcm}^{-2}} \right)^{-1} \left(\frac{\sigma_{pp}}{100 \text{mb}} \right)^{-1}$.

The CRs escape from the GRB host galaxy in two ways. One is advective transportation by the galactic wind. Galactic-scale gaseous winds are ubiquitous in star-forming galaxies at all cosmic epochs (Heckman et al. 1990; Pettini et al. 2001; Shapley et al. 2003). Such winds can be driven by stellar winds, supernova explosions or other processes. It is found that, for luminous and ultraluminous infrared galaxies at low redshifts, the winds from more luminous starbursts have higher speeds, roughly as $v_w \propto \text{SFR}^k$ with k being in the range of 0.25-0.35 (Martin 2005; Rupke et al. 2005; Arribas et al. 2014). A similar trend is found for star-forming galaxies at $z \sim 1$ (Weiner et al. 2009), i.e.

$$v_w \approx 175 \left(\frac{\text{SFR}}{1 M_{\odot} \text{yr}^{-1}} \right)^{0.3}, \quad (5)$$

with the error in v_w being 35%. Such type of relation between the velocity of the outflowing material and SFR is expected if the mechanical energy is supplied by stellar winds and supernova explosions. Thus, one can calculate v_w for each GRB hosts with measured N_H under the help of Eq. 4 and Eq. 5. Taking $v_w = 500 \text{km s}^{-1}$ as the reference value for GRB host galaxies, the advective escape time is $t_{\text{adv}} = l/v_w = 9 \times 10^5 \text{yr} \frac{l}{500 \text{pc}} \left(\frac{v_w}{500 \text{kms}^{-1}} \right)^{-1}$.

The other way that CRs escape is diffusion, i.e., CRs are scattered off small-scale magnetic field inhomogeneities randomly and diffuse out of the host galaxy. The diffusion time is estimated to be $t_{\text{diff}} = l^2/4D$, where $D = D_0 (E/E_0)^{\delta}$ is the diffusion coefficient, and D_0 and $E_0 = 3 \text{GeV}$ are normalization factors. Since little is known about the diffusion coefficient in GRB host galaxies, in the calculation we allow lower diffusion coefficients than that of our Galaxy, which is $D_0 = 10^{28} \text{cm}^2 \text{s}^{-1}$. The energy dependence of the diffusion coefficient is also unknown and $\delta = 0-1$ depending on the spectrum of interstellar magnetic turbulence. We assume two cases, one is the commonly-used value $\delta = 0.5$, based on the measurement of the CR confinement time in our Galaxy (Engelmann et al. 1990; Webber et al. 2003). Another choice is $\delta = 0.3$, assuming the Kolmogorov-type turbulence. Then the diffusive

escape time is $t_{\text{diff}} = 10^4 \text{yr} \left(\frac{l}{500 \text{pc}} \right)^2 \left(\frac{D_0}{10^{26} \text{cm}^2 \text{s}^{-1}} \right)^{-1} \left(\frac{\varepsilon_p}{60 \text{PeV}} \right)^{-0.3}$, with $\varepsilon_p \simeq 25(1+z)\varepsilon_\nu$.

Combining the advective and diffusive escape timescales, the total escape time is $t_{\text{esc}}^{-1} = t_{\text{diff}}^{-1} + t_{\text{adv}}^{-1}$. When the difference between t_{loss} and t_{adv} is large, $t_{\text{esc}} \approx \min(t_{\text{diff}}, t_{\text{adv}})$. Note that when $t_{\text{adv}} \ll t_{\text{diff}}$, which holds for low-energy CRs and small values of D_0 , the pion production efficiency is independent of l and is given by

$$f_\pi \simeq 0.17 \left(\frac{\Sigma_g}{0.01 \text{gcm}^{-2}} \right) \left(\frac{v_w}{500 \text{kms}^{-1}} \right)^{-1} \left(\frac{\sigma_{pp}}{100 \text{mb}} \right). \quad (6)$$

The dependence of f_π on CR energy has a break at the energy where $t_{\text{adv}} = t_{\text{diff}}$. Below the break energy, f_π slightly increases with the energy due to the pp -collision inelastic cross-section, while above the break f_π decreases as $\varepsilon_p^{-\delta}$, leading to a steeper neutrino spectrum.

3.2. Calibration of CR flux from GRBs

The Fermi/GBM detection rate of GRBs is about 250 per year (Paciesas et al. 2012), and the total gamma-ray (10-1000 keV) fluence of GRBs detected in one year is $2 \times 10^{-3} \text{ergcm}^2$. The GBM field of view (FOV) is roughly $\Omega_{\text{GBM}} = 2\pi$ steradians, so the total all-sky flux of gamma-rays in 10-1000 keV is $F_\gamma = 4 \times 10^{-3} \text{ergcm}^{-2} \text{yr}^{-1}$. Then the energy production rate of gamma-rays in the energy range of 10-1000 keV, is estimated to be $W_\gamma(z=0) = \xi F_\gamma H/c = 5 \times 10^{42} (\xi/0.5) \text{ergMpc}^{-3} \text{yr}^{-1}$, where H is the Hubble constant and ξ is a factor accounting for the source density evolution with redshift (Eichler et al. 2010). According to the estimate of Katz et al. (2009), the present-day differential energy production rate of UHE-CRs above 30 EeV is $\varepsilon_p^2 d\dot{n}/d\varepsilon_p(z=0) = (0.45 \pm 0.15)(\alpha-1) \times 10^{44} \text{ergMpc}^{-3} \text{yr}^{-1}$, where α is the power-law index of the CR spectrum. We assume $\alpha = 2$ as suggested by Fermi acceleration. Define η_p as the ratio between the differential energy production rate of UHECRs and the energy production rate of gamma-rays in 10-1000 keV. If GRBs are the source of UHE-CRs above 30 EeV, $\eta_p = (\varepsilon_p^2 d\dot{n}/d\varepsilon_p)/W_\gamma(10-1000 \text{KeV}) = 9 \pm 3$, assuming $\xi = 0.5$ (Eichler et al. 2011).

3.3. The neutrino flux

We collect a sample of GRBs that have both measurements of N_H and gamma-ray fluence. As the energy coverage of Swift BAT is small, we choose GRBs that are detected by Fermi/GBM to get more accurate values of the gamma-ray fluence. There are 45 GRBs in total that have measurements of both N_H and gamma-ray fluence, as shown in Table 2. For each GRB, the (single-flavor) neutrino fluence is estimated to be

$$\varepsilon_\nu^2 \Phi_\nu = \frac{1}{6} f_\pi \varepsilon_p^2 \phi_p = \frac{1}{6} f_\pi \eta_p F_\gamma, \quad (7)$$

where $\varepsilon_p^2 \phi_p$ is the differential energy flux of CR protons and F_γ is the gamma-ray fluence of this GRB. The accumulated neutrino flux produced by all GRBs in the universe is

$$\varepsilon_\nu^2 \Phi_\nu = \frac{1}{N} \sum_i \varepsilon_\nu^2 \phi_{\nu,i} R_{\text{GRB}} (4\pi)^{-1} \quad (8)$$

where i represents the i th GRB in our sample, N is the total number of GRBs in our sample, and $R_{\text{GRB}} = 500 \text{yr}^{-1}$ is the all-sky rate of GRBs that would be detected by Fermi/GBM if the field of view of GBM is 4π steradians. The result of the accumulated neutrino flux is shown in Fig.2. We

find that the accumulated neutrino flux at PeV is $(0.3 \pm 0.2) \times 10^{-8} \text{GeV cm}^{-2} \text{yr}^{-1} \text{sr}^{-1}$ per flavor for $\delta = 0.3$ and $D_0 = 10^{26} \text{cm}^2 \text{s}^{-1}$. The 1 sigma error in the accumulated flux is obtained by using formulas for the propagation of error. It results mainly from the uncertainties in the neutrino production efficiency f_π , in the values of N_H , and in the CR-to-gamma-ray ratio η_p .

Since the CR diffusion coefficient is not well-understood, we study its effect on the neutrino flux. The results for different values of δ and D_0 are shown in Fig. 3. One can see that, when D_0 decreases, the neutrino flux increases at PeV energies. For $\delta = 0.3$, if D_0 is as low as $10^{25} \text{cm}^2 \text{s}^{-1}$, the neutrino spectrum becomes too hard, although the flux increases. For $\delta = 0.5$, lower values of D_0 is needed to produce the same flux compared to the case of $\delta = 0.3$. However, the confinement of 100 PeV CRs producing PeV neutrinos requires that D_0 be larger than $10^{24} \text{cm}^2 \text{s}^{-1}$ (Murase et al. 2013). Thus, even under favorable conditions about the CR diffusion coefficient, the neutrino flux produced by GRB CRs alone can not explain the IceCube observations if other assumptions used in our calculation are correct.

In the calculation of the accumulated neutrino flux, we only considered those GRBs that triggered Fermi/GBM detector (i.e. adopting $R_{\text{GRB}} = 500 \text{yr}^{-1}$). There are dim GRBs that do not trigger the detector and their total gamma-ray fluence may even be larger than that of the triggered ones according to the simulation results in Liu & Wang (2013). These untriggered GRBs may also produce diffuse neutrinos as triggered GRBs. However, one should note that considering the contribution by untriggered GRBs would not change our result about the accumulated neutrino flux, because the CR-to-gamma-ray ratio η_p needs to be re-calibrated correspondingly and thus the accumulated neutrino flux remains unchanged.

There could be an exceptional case, i.e., if some dim GRBs do not accelerate protons to energy 10^{19}eV (although nuclei can still be accelerated to ultra high energies), but they can still contribute to PeV neutrinos with CRs of $\gtrsim 100 \text{PeV}$. Note also that this does not exclude the possibility that low-luminosity GRBs themselves are responsible for their origin (e.g., Murase & Ioka 2013, Bhattacharya et al. 2014).

4. DISCUSSIONS AND CONCLUSIONS

The above calculation has some uncertainties in the following aspects. First, the estimate of the energy production rate of gamma-rays W_γ has uncertainty (e.g., Dermer 2012). Note that the factor $\xi = 0.5$ is obtained by assuming that GRB rate follows the cosmic SFR of Porciani & Madau (2001) or that of Hopkins & Beacom (2008). If GRB density evolves faster than the cosmic SFR, ξ is smaller and then η_p is larger. Second, the estimate of the UHECR energy budget has uncertainty. The value can be a bit larger if one uses the Telescope Array or HiRes data. Third, the power-law index α could be softer than 2, then the energy budget of CRs at 100 PeV could be larger. Thus, given these uncertainties, the neutrino flux in the optimistic case could reach the observed value of IceCube.

On the other hand, if one consider that GRB host galaxies that are not detected by optical observations are possibly smaller galaxies, such as dwarf galaxies, the pion production efficiency may be smaller and thus the neutrino flux contributed by these galaxies would be smaller. Also, as shown by Eq. 6, the pion production efficiency depends on the speeds of the galactic winds. The properties of the galactic winds in GRB host galaxies are not well-explored. X-ray observations of starburst galactic winds, such as M82, usually give a

higher speeds than that inferred from the optical observations (Strickland & Heckman 2009). If the galactic wind speeds of GRB hosts are proven to be higher, the neutrino flux produced by GRB hosts would decrease. The pion production efficiency also depends on the diffusive coefficient. If D_0 is larger than $10^{27} \text{ cm}^2 \text{ s}^{-1}$ (for example, $D_0 = 10^{28} \text{ cm}^2 \text{ s}^{-1}$ for our Galaxy), the accumulated neutrino flux would be lower than $10^{-9} \text{ GeV cm}^{-2} \text{ yr}^{-1} \text{ sr}^{-1}$ at 1 PeV, as shown in Fig. 3.

In summary, we calculated the neutrino flux produced by CRs accelerated by GRBs while they are propagating in the host galaxies based on our current knowledge about GRB and their host galaxies. These CRs collide with nuclei of ISM and produce neutrinos before they escape out of the galaxy. When the flux of CRs produced by GRBs is normalized with the observed flux of UHECRs above $\sim 10^{19} \text{ eV}$, the accumulated

neutrino flux is $(0.3 \pm 0.2) \times 10^{-8} \text{ GeV cm}^{-2} \text{ s}^{-1} \text{ sr}^{-1}$ per flavor under the usual assumptions about the GRB properties and favorable assumptions about the CR diffusion coefficient. The estimate, however, has uncertainty due to uncertainty in our current knowledge of GRB and their host galaxies and the accumulated neutrino flux could reach the observed value by IceCube in the optimistic case, so we can not rule out this scenario at present.

We thank Zhuo Li and Ruoyu Liu for useful discussions. This work is supported by the 973 program under grant 2014CB845800, the NSFC under grants 11273016 and 11033002, and the Excellent Youth Foundation of Jiangsu Province (BK2012011).

REFERENCES

- Aartsen, M. G., Ackermann, M., Adams, J., et al. 2014, *Physical Review Letters*, 113, 101101
- Aartsen, M. G., et al. 2015, arXiv:1412.6510
- Abbasi, R. et al. *Nature*, 484, 351
- Arnaud, K. A. 1996, *Astronomical Data Analysis Software and Systems V*, 101, 17
- Arribas, S. et al. 2014, arXiv:1404.1082
- Bhattacharya, A., Enberg, R., Hall Reno, M., & Sarcevic, I. 2014, arXiv:1407.2985
- Dermer, C. D., & Atoyan, A. 2006, *New Journal of Physics*, 8, 122
- Dermer, C. D., 2014, arXiv: 1202.2814
- Eichler, D., Guetta, D., & Pohl, M. 2010, *ApJ*, 722, 543
- Engelmann, J. J., Ferrando, P., Soutoul, A., Goret, P., & Juliusson, E. 1990, *A&A*, 233, 96
- Fruchter, A. S., Levan, A. J., Strolger, L., et al. 2006, *Nature*, 441, 463
- Guetta, D., & Granot, J. 2004, *Gamma-Ray Bursts in the Afterglow Era*, 312, 377
- He, H.-N., Liu, R.-Y., Wang, X.-Y., et al. 2012, *ApJ*, 752, 29
- Heckman, T. M., Armus, L., & Miley, G. K. 1990, *ApJS*, 74, 833
- Hopkins, A. M., & Beacom, J. F. 2006, *ApJ*, 651, 142
- Isobe, T., Feigelson, E. D., Akritas, M. G., & Babu, G. J. 1990, *ApJ*, 364, 104
- Katz, B., Budnik, R., & Waxman, E. 2009, *JCAP*, 3, 020
- Katz, B., Waxman, E., Thompson T., Loeb, A., 2013, arXiv:1311.0287
- Kelner, S. R., Aharonian, F. A., & Bugayov, V. V. 2006, *Phys. Rev. D*, 74, 034018
- Kelly, P. et al., 2014, arXiv: 1401.0729
- Kennicutt, R. C., Jr. 1998, *ApJ*, 498, 541
- Liu, R.-Y., & Wang, X.-Y. 2013, *ApJ*, 766, 73
- Martin, C. L. 2005, *ApJ*, 621, 227
- Milgrom, M., & Usov, V. 1995, *ApJ*, 449, L37
- Murase, K., Ahlers, M., & Lacki, B. C. 2013, *Phys. Rev. D*, 88, 121301
- Murase, K., Ioka, K., Nagataki, S., & Nakamura, T. 2006, *ApJ*, 651, L5
- Murase, K., & Ioka, K. 2013, *Physical Review Letters*, 111, 121102
- Paciesas, W. S., 2012, *ApJS*, 199, 18
- Pettini, M., Shapley, A. E., Steidel, C. C., et al. 2001, *ApJ*, 554, 981
- Porciani, C., & Madau, P. 2001, *ApJ*, 548, 522
- Prieto, J. L. Stanek K. Z., and Beacom J. F., 2008, *Astrophys. J.* 673, 999
- Rupke, D. S., Veilleux, S., & Sanders, D. B. 2005, *ApJS*, 160, 115
- Savaglio, S., Glazebrook, K., & Le Borgne, D. 2009, *ApJ*, 691, 182
- Shapley, A. E., Steidel, C. C., Adelberger, K. L., & Pettini, M. 2003, *Revista Mexicana de Astronomia y Astrofisica Conference Series*, 17, 254
- Stanek K. Z. et al. 2006; *Acta Astron.* 56, 333
- Strickland, D. K., & Heckman, T. M. 2009, *ApJ*, 697, 2030
- Svensson, K. M., Levan, A. J., Tanvir, N. R., Fruchter, A. S., & Strolger, L.-G. 2010, *MNRAS*, 405, 57
- Vietri, M. 1995, *ApJ*, 453, 883
- Wang, B., Zhao, X., & Li, Z. 2014, *JCAP*, 11, 028
- Wang, X.-Y., & Dai, Z.-G. 2009, *ApJ*, 691, L67
- Waxman, E. 2013, arXiv:1312.0558
- Waxman, E. 1995, *Physical Review Letters*, 75, 386
- Waxman, E., & Bahcall, J. 1997, *Physical Review Letters*, 78, 2292
- Webber, W. R., McDonald, F. B., & Lukasiak, A. 2003, *ApJ*, 599, 582
- Weiner, B. J., Coil, A. L., Prochaska, J. X., et al. 2009, *ApJ*, 692, 187
- Yacobi, L.; Guetta, D.; Behar, E., 2014, *ApJ*, 793, 48
- Zhang, B., & Kumar, P. 2013, *Physical Review Letters*, 110, 121101

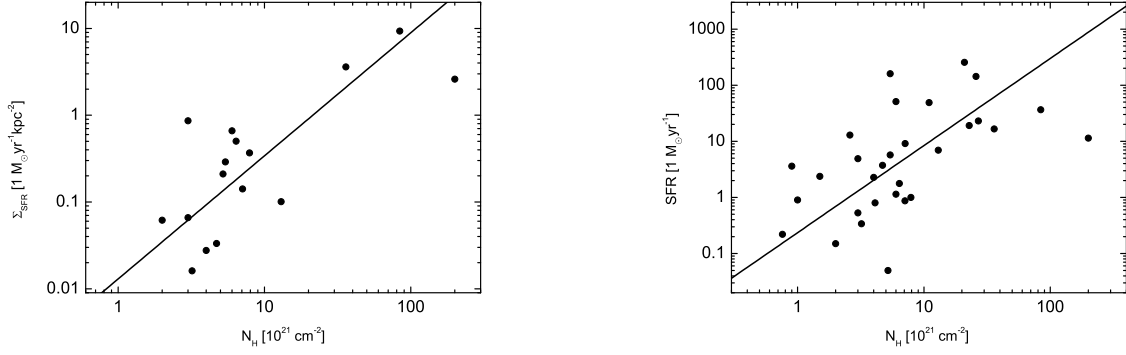


FIG. 1.— Left panel: the relation between the surface star-formation rate Σ_{SFR} and the X-ray absorption column density N_{H} . Right panel: the relation between the total star-formation rate SFR and the X-ray absorption column density N_{H} . The data points are from table 1. The lines represent the best OLS bisector fits. See the text for more details.

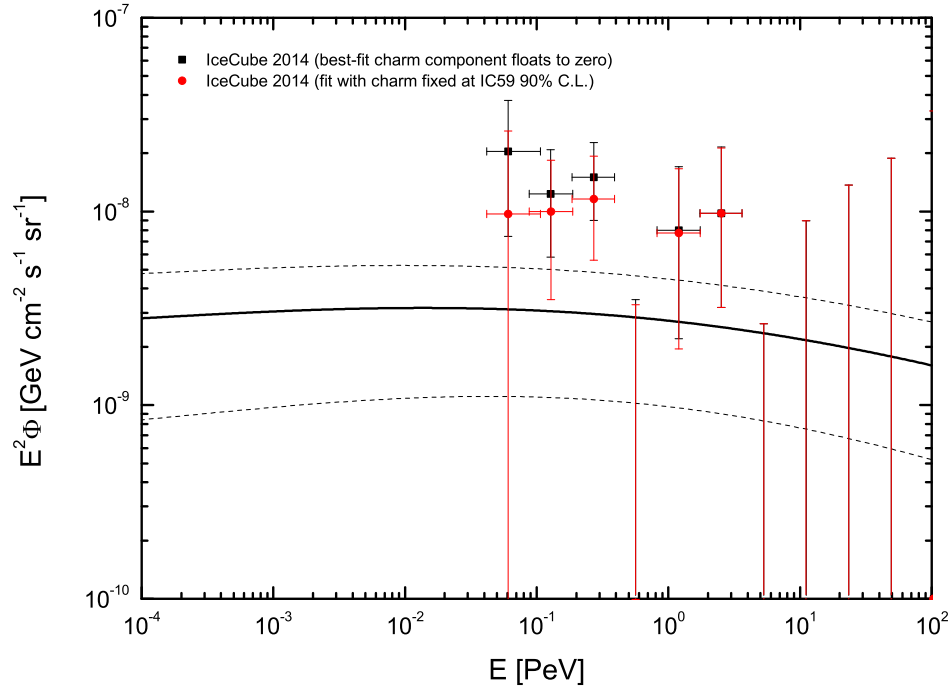


FIG. 2.— The energy spectra of neutrino emission in comparison with IceCube data. The solid line represents the neutrino flux obtained using $\delta = 0.3$ and $D_0 = 10^{26} \text{ cm}^2 \text{ s}^{-1}$, and the dashed lines are the $1-\sigma$ error. The IceCube data are also shown.

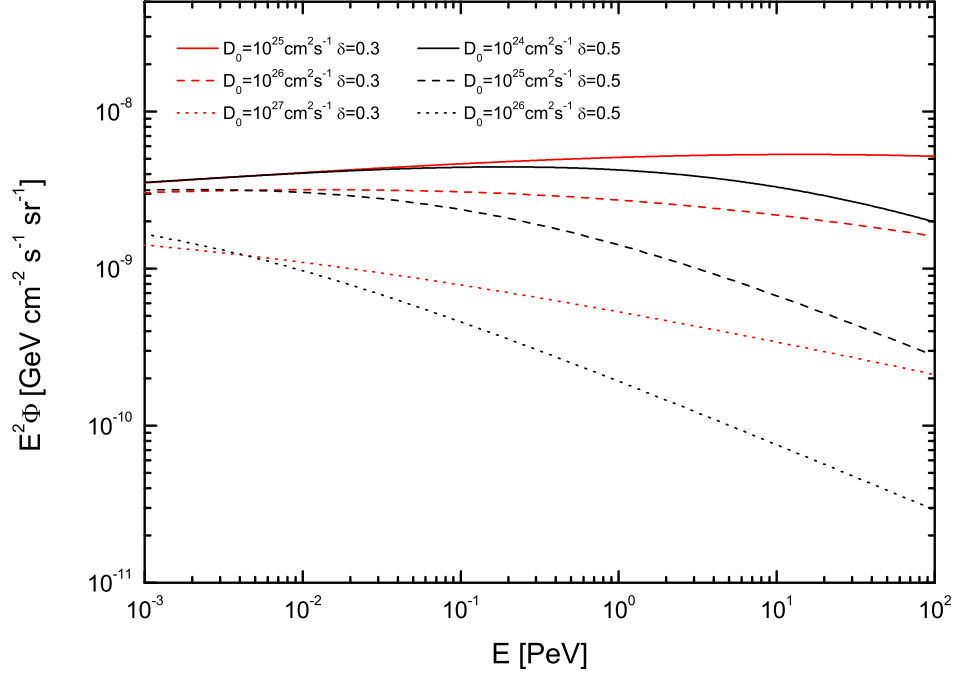


FIG. 3.— The energy spectra of neutrino emission for different values of δ and D_0 .

TABLE 1
GALAXY PARAMETERS OF GRB HOSTS

GRB	SFR [$M_{\odot} \text{ yr}^{-1}$]	N_H [10^{21} cm^{-2}]	R_{80} [kpc]	Ref.
GRB 050826	9.13	$7.1^{+2.0}_{-2.0}$	-	[1,2]
GRB 051006	51	6^{+3}_{-3}	-	[3,A]
GRB 060814	256	$20.9^{+2.3}_{-2.2}$	-	[3,4]
GRB 061121	160	$5.4^{+0.8}_{-0.5}$	-	[3,4]
GRB 061126	2.38	$1.5^{+0.2}_{-0.2}$	-	[1,A]
GRB 070306	143	$26.8^{+4.7}_{-4.3}$	-	[3,4]
GRB 080325	12.9	$2.6^{+0.1}_{-0.1}$	-	[5,A]
GRB 080607	19.1	$22.8^{+4.7}_{-5.2}$	-	[5,4]
GRB 081109	49.0	$11^{+1.3}_{-1.2}$	-	[5,6]
GRB 090328	4.8	$0.9^{+1.1}_{-0.9}$	-	[7,A]
GRB 090424	0.8	$4.1^{+0.6}_{-0.5}$	-	[8,4]
GRB 091127	0.22	$0.76^{+0.35}_{-0.5}$	-	[9,4]
GRB 120624B	23	27^{+46}_{-26}	-	[10,11]
GRB 130427	0.9	$1.0^{+0.1}_{-0.1}$	-	[10,12]
GRB 970228	0.53	3^{+6}_{-4}	3.2	[1,13,14]
GRB 970508	1.14	6^{+10}_{-5}	1.48	[1,13,14]
GRB 970828	0.87	$7.08^{+3.21}_{-2.75}$	2.8	[1,15,14]
GRB 971214	11.4	200^{+290}_{-120}	2.36	[1,13,14]
GRB 980703	16.57	36^{+22}_{-13}	2.42	[1,13,14]
GRB 990123	5.72	$5.4^{+9.4}_{-2.7}$	5.01	[1,13,14]
GRB 990705	6.96	13	9.38	[1,16,14]
GRB 000926	2.28	$4^{+3.5}_{-2.5}$	10.25	[1,17,14]
GRB 011211	4.90	$3.0^{+1.1}_{-1.1}$	2.69	[1,18,14]
GRB 020405	3.74	$4.7^{+3.7}_{-3.7}$	11.96	[1,19,14]
GRB 030323	1	$7.9^{+1.4}_{-1.2}$	1.86	[20,20,14]
GRB 041006	0.34	$3.2^{+0.16}_{-0.16}$	5.19	[1,17,14]
GRB 050416A	1.77	$6.4^{+0.9}_{-0.5}$	2.12	[21,4,21]
GRB 050525A	0.15	$2.0^{+0.9}_{-0.9}$	1.76	[21,4,21]
GRB 051022	36.46	$83.9^{+8.5}_{-7.8}$	2.23	[1,5,21]
GRB 060218	0.05	$5.2^{+0.5}_{-0.3}$	0.55	[1,2,21]

(1)Savaglio, S., et al. 2009, ApJ, 691, 182 (2)Campana, S., et al. 2010, MNRAS, 402, 2429 (3)Perley, D. A., et al. 2014, arXiv:1407.4456 (4)Campana, S., et al. 2012, MNRAS, 421, 1697 (5)Perley, D. A., et al. 2013, ApJ, 778, 128 (6)Krühler, T., et al. 2011, A&A, 534, AA108 (7)McBreen, S., et al. 2010, A&A, 516, AA71 (8)Jin, Z.-P., et al. 2013, ApJ, 774, 114 (9)Vergani, S. D., et al. 2011, A&A, 535, AA127 (10)Wang, F. Y., & Dai, Z. G. 2014, ApJS, 213, 15 (11)de Ugarte Postigo, A., et al. 2013, A&A, 557, LL18 (12)Littlejohns, O. M., et al. 2014, arXiv:1412.6530 (13)Galama, T. J., & Wijers, R. A. M. J. 2001, ApJ, 549, L209 (14)Svensson, K. M., 2010, MNRAS, 405, 57 (15)Yoshida, A., et al. 2001, ApJ, 557, L27 (16)Amati, L., et al. 2000, Science, 290, 953 (17)Kann, D. A., et al. 2006, ApJ, 641, 993 (18)Reeves, J. N., et al. 2003, A&A, 403, 463 (19)Covino, S., et al. 2003, A&A, 400, L9 (20)Vreeswijk, P. M., et al. 2004, A&A, 419, 927 (21)Fruchter, A. S., et al. 2006, Nature, 441, 463 (A) is from the GCN website.

TABLE 2
THE X-RAY ABSORPTION COLUMN DENSITY AND 10-1000KeV FLUENCE

GRB	N_H^a [10^{21} cm^{-2}]	GBM Fluence ^b [erg/cm ²]	z^a
141004A	$1_{-1}^{+1.5}$	1.18×10^{-6}	0.57
140907A	$0.7_{-0.6}^{+0.7}$	6.45×10^{-6}	1.21
140703A	$5.4_{-5.4}^{+8}$	7.62×10^{-6}	3.14
140512A	$0.52_{-0.26}^{+0.28}$	2.93×10^{-5}	0.725
140506A	$1.8_{-0.4}^{+0.4}$	6.59×10^{-6}	0.889
140423A	$6.6_{-3}^{+3.2}$	1.81×10^{-5}	3.26
140304A	$0.38_{-0.31}^{+0.34}$	2.24×10^{-6}	5.28
140213A	$1.4_{-0.9}^{+1}$	2.12×10^{-5}	1.2076
140206A	$10.1_{-2.3}^{+2.4}$	1.55×10^{-5}	2.74
131105A	$1.7_{-1.2}^{+1.4}$	2.38×10^{-5}	1.686
130612A	$7.7_{-5.5}^{+6.6}$	6.80×10^{-7}	2.006
130610A	$2.6_{-2.6}^{+2.8}$	3.54×10^{-6}	2.092
130420A	$0.58_{-0.24}^{+0.25}$	1.16×10^{-5}	1.297
121211A	$4.59_{-0.99}^{+1.07}$	6.41×10^{-7}	1.023
121128A	11_{-4}^{+5}	9.30×10^{-6}	2.2
120922A	$0.236_{-0.27}^{+0.28}$	8.21×10^{-6}	3.1
120907A	$0.46_{-0.29}^{+0.31}$	8.09×10^{-7}	0.97
120811C	$0.67_{-0.31}^{+0.34}$	3.45×10^{-6}	2.67
120729A	$0.7_{-0.4}^{+0.5}$	5.08×10^{-6}	0.8
120712A	$0.14_{-0.14}^{+0.31}$	4.43×10^{-6}	4.1
120326A	$0.39_{-0.22}^{+0.23}$	3.26×10^{-6}	1.798
120119A	$1.3_{-0.4}^{+0.5}$	3.87×10^{-5}	1.73
111228A	$2.51_{-0.47}^{+0.49}$	1.81×10^{-5}	0.715
111107A	$3.5_{-3.5}^{+6}$	9.07×10^{-7}	2.893
110818A	$0.52_{-0.24}^{+0.27}$	5.15×10^{-6}	3.36
110213A	$0.61_{-0.23}^{+0.24}$	9.37×10^{-6}	1.46
110128A	~ 0	1.43×10^{-6}	2.339
101219B	$0.5_{-0.5}^{+0.7}$	3.99×10^{-6}	0.5519
100906A	$8.1_{-2.5}^{+2.5}$	2.33×10^{-5}	1.727
100816A	$2.6_{-1.1}^{+1.1}$	3.65×10^{-6}	0.8039
100814A	1.6	1.49×10^{-5}	1.44
100728B	$4.3_{-2.5}^{+3.1}$	3.34×10^{-6}	2.1
100728A	$2.7_{-0.3}^{+0.3}$	1.28×10^{-4}	1.567
100704A	$2.1_{-0.8}^{+0.9}$	1.04×10^{-5}	3.6
100615A	$11_{-1.2}^{+1.3}$	8.72×10^{-6}	1.398
091208B	$8.3_{-3.4}^{+4.3}$	6.19×10^{-6}	1.063
091127	$0.76_{-0.5}^{+0.35}$	2.07×10^{-5}	0.49
091020	$5.8_{-1.6}^{+1.7}$	8.35×10^{-6}	1.71
090926B	$13.9_{-1.5}^{+1.6}$	1.08×10^{-5}	1.24
090516A	$22.9_{-3.9}^{+4}$	1.72×10^{-5}	4.1
090424	$4.1_{-0.5}^{+0.6}$	4.63×10^{-5}	0.544
090423	102_{-54}^{+49}	8.16×10^{-7}	8
081221	$26.1_{-3.6}^{+3.8}$	3.00×10^{-5}	2.26
080916A	$8_{-1.9}^{+3.2}$	7.81×10^{-6}	0.689
080905B	$22.6_{-4.7}^{+5.3}$	2.91×10^{-6}	2.374

(a)From the GCN website. (b)From Fermi-GBM GRB list of detections. <http://www.asdc.asi.it/grbgbm/>